

# Crystal structure of human 53BP1 BRCT domains bound to p53 tumour suppressor

Dean J. Derbyshire, Balaku P. Basu,  
Louise C. Serpell, Woo S. Joo<sup>1</sup>,  
Takayasu Date<sup>2</sup>, Kuniyoshi Iwabuchi<sup>2</sup> and  
Aidan J. Doherty<sup>3</sup>

Structural Medicine Unit, Cambridge Institute for Medical Research and Department of Haematology, University of Cambridge, Hills Road, Cambridge CB2 2XY, UK, <sup>1</sup>Cellular Biochemistry and Biophysics Program, Memorial Sloan-Kettering Cancer Center, New York, NY 10021, USA and <sup>2</sup>Department of Biochemistry, Kanazawa Medical University, Ishikawa 920-0293, Japan

<sup>3</sup>Corresponding author  
e-mail: ajd42@cam.ac.uk

**The BRCT (BRCA1 C-terminus) is an evolutionary conserved protein–protein interacting module found as single, tandem or multiple repeats in a diverse range of proteins known to play roles in the DNA-damage response. The BRCT domains of 53BP1 bind to the tumour suppressor p53. To investigate the nature of this interaction, we have determined the crystal structure of the 53BP1 BRCT tandem repeat in complex with the DNA-binding domain of p53. The structure of the 53BP1–p53 complex shows that the BRCT tandem repeats pack together through a conserved interface that also involves the inter-domain linker. A comparison of the structure of the BRCT region of 53BP1 with the BRCA1 BRCT tandem repeat reveals that the interdomain interface and linker regions are remarkably well conserved. 53BP1 binds to p53 through contacts with the N-terminal BRCT repeat and the inter-BRCT linker. The p53 residues involved in this binding are mutated in cancer and are also important for DNA binding. We propose that BRCT domains bind to cellular target proteins through a conserved structural element termed the ‘BRCT recognition motif’.**

**Keywords:** 53BP1/BRCA1/BRCT/DNA repair/p53

## Introduction

DNA damage triggers a variety of cellular responses in eukaryotic cells, including the induction of a regulatory signalling network that activates DNA-repair pathways. DNA-repair proteins are highly diverse structurally, but many have been shown to contain a conserved globular domain, first identified in the breast cancer tumour suppressor protein BRCA1 and thus designated BRCT (BRCA1 C-terminus) (Bork *et al.*, 1997; Callebaut and Mornon, 1997). The BRCT domain consists of ~95 amino acid residues and has been observed as single, tandem or multiple repeats in a multitude of proteins of different apparent functions. The structures of the single BRCT domains of XRCC1 (Zhang *et al.*, 1998) and ligase III

(Krishnan *et al.*, 2001) and the tandem repeat of BRCA1 (Williams *et al.*, 2001) have been reported. The BRCT domain consists of a four-stranded parallel  $\beta$ -sheet flanked by three  $\alpha$ -helices. BRCT-containing proteins are known to play roles (directly or indirectly) in DNA-damage response, including cell-cycle control and checkpoint-mediated repair. This includes proteins such as BRCA1, 53BP1, RAD9, Rad4, ECT2, XRCC1, RAPI, terminal transferases, poly(ADP-ribose) polymerases and DNA ligases III and IV (Bork *et al.*, 1997; Callebaut and Mornon, 1997). Despite the overall functional diversity of these BRCT-containing proteins, participation in the DNA-damage response appears to be a unifying theme. Furthermore, BRCT domains are likely to perform critical functions in the cell-cycle control of organisms from bacteria to humans. It is believed that BRCT modules can interact in various ways forming either homo- or hetero-BRCT dimers and complexes with non-BRCT proteins (Huyton *et al.*, 2000), as well as complexes with DNA (Yamane and Tsuruo, 1999). It has been suggested that BRCT domains may act as signal transducers that transmit the signals from DNA-damage detectors to other components of the DNA-repair machinery via specific protein–protein interactions (Bork *et al.*, 1997). The BRCT domain of mammalian DNA ligase III forms a specific complex with the C-terminal BRCT domain of XRCC1 (Nash *et al.*, 1997), and DNA ligase IV, shown to be important in double-strand break repair, interacts with XRCC4 via a BRCT tandem repeat (Critchlow *et al.*, 1997; Grawunder *et al.*, 1997). These examples provide direct evidence that BRCT domains physically mediate contacts between components of the DNA-repair machinery. The C-terminal BRCT domain of BRCA1 corresponds precisely to the minimal transcription activation domain of this protein (Chapman and Verma, 1996), indicating another possible function for BRCT domains.

A two-hybrid screen has shown that the BRCT-containing protein, p53-binding protein 1 (53BP1) binds to wild-type p53 but fails to bind to mutant p53, suggesting that it may be involved in the ability of wild-type p53 to suppress transformation (Iwabuchi *et al.*, 1994). The tumour suppressor protein p53 plays a critical role in many key cellular processes (Lane, 1992; Levine, 1993), acting as a transcriptional activator for a number of DNA damage and growth arrest genes, as well as negatively regulating the transcription of genes that have TATA box-initiated promoters, and is thought to be involved directly in checking both viral and eukaryotic DNA replication (Horikoshi *et al.*, 1995). p53 binds as a tetramer to response elements through a sequence-specific DNA-binding core domain extending from amino acid residues 96–308 (Pavletich *et al.*, 1993). Studies of tumour-derived p53 mutants have shown that they are defective in sequence-specific DNA-binding and, consequently, cannot

activate transcription (Hollstein *et al.*, 1991). These studies strongly suggest that sequence-specific DNA binding and transactivation are the key biochemical activities responsible for much of the biological function of p53. Mutations in the p53 protein have been associated with human cancers and the vast majority of these mutations are located in the DNA-binding core domain (Pavletich *et al.*, 1993) and affect its sequence-specific DNA-binding activity (Cho *et al.*, 1994). This suggests that p53 function is mediated by its DNA-binding and transactivation properties (Bargonetti *et al.*, 1993; Pavletich *et al.*, 1993). The co-crystal structure of the p53 nucleoprotein complex has provided valuable insights into the binding specificity of p53 by identifying specific binding contacts (Cho *et al.*, 1994).

It has been reported that 53BP1 binds to the DNA-binding domain of p53 and enhances p53-mediated transcriptional activation (Iwabuchi *et al.*, 1994). The C-terminal region of 53BP1 interacts with p53 and sequence analysis has shown that this region contains a BRCT tandem repeat (Iwabuchi *et al.*, 1998). It has been reported recently that after DNA damage, 53BP1 relocalizes to discrete nuclear foci that are thought to represent sites of DNA lesions and becomes hyperphosphorylated (Schultz *et al.*, 2000; Anderson *et al.*, 2001; Rappold *et al.*, 2001; Xia *et al.*, 2001). 53BP1 is readily phosphorylated *in vitro* whilst ataxia-telangiectasia mutated kinase (ATM)-deficient cells show no 53BP1 hyperphosphorylation and reduced 53BP1 foci formation in response to  $\gamma$ -radiation compared with cells expressing wild-type ATM. These results suggest that 53BP1 is a target substrate for ATM and is involved early in the DNA-damage signalling pathways in mammalian cells. A recent report suggests that 53BP1 may also have a distinct role in checkpoint signalling during mitosis (Jullien *et al.*, 2002). It has been shown that the C-terminal BRCT domain of BRCA1 also interacts with the p53 DNA-binding domain both *in vivo* and *in vitro*, and stimulates transcription (Chai *et al.*, 1999). This suggests possible parallels between the functioning of BRCA1 and 53BP1.

To investigate the nature of the molecular interactions between 53BP1 and p53, we have determined the 2.6 Å crystal structure of the DNA-binding domain of p53 in complex with the predicted BRCT tandem repeat of 53BP1. In this report, we have elucidated the structural basis for the interactions of BRCT domains with p53. A comparison of the structure of the 53BP1 BRCT domains with other BRCTs in the Protein Data Bank (PDB), including the human BRCA1 tandem repeat, shows that they have remarkably similar structures and provides important insights into the molecular basis for protein-protein contacts mediated by BRCT domains.

## Results and discussion

Iwabuchi *et al.* (1998) reported that 53BP1 interacts with the DNA-binding domain of p53 via two C-terminal BRCT domains. We have defined the minimal region of 53BP1, containing a tandem repeat of BRCT domains, that interacts directly with the core domain of p53 (Derbyshire *et al.*, 2002). We produced a series of N-terminal truncated forms of 53BP1 to define the most stable interacting domain of 53BP1. These truncated proteins were

**Table I.** Data collection and structure statistics

X-ray source	CuK $\alpha$
Wavelength (Å)	1.541
Cell dimensions: <i>a</i> ; <i>b</i> ; <i>c</i> (Å), <i>P</i> <sub>21</sub> 2 <sub>1</sub> 2 <sub>1</sub>	71.52; 94.57; 136.20
Resolution range (Å)	55.0–2.6
% Completeness	99.1 (96.9)
Multiplicity	7.7 (3.70)
<i>R</i> <sub>sym</sub>	10.4 (35.8)
<i>I</i> / $\sigma$ ( <i>I</i> )	6.2 (1.40)
<i>R</i> -factor/correlation <sup>a</sup>	51.1/41.02
<i>R</i> -factor/correlation <sup>b</sup>	42.2/66.01
<i>V</i> <sub>M</sub> /% solvent	2.13/41.76
Resolution range (Å)	500–2.6
No. reflections (working)	51 284 (93.4% of theoretical)
No. reflections (free)	2835 (5.20% of theoretical)
No. non-hydrogen atoms	6510
No. waters	110
No. SO <sub>4</sub> ions	2
R.m.s.ds from ideality:	
Bond lengths (Å)	0.00782
Bond angles (°)	1.34850
Average temperature factors:	
Protein	37.30
Water	31.06
SO <sub>4</sub> ions	48.76
<i>R</i> -factor/ <i>R</i> <sub>free</sub>	23.81/28.83
Ramachandran plot:	
% Most favoured regions	85.9
% Additionally allowed regions	14.1
Overall <i>G</i> -factor	0.24

<sup>a</sup>p53 partial structure from AMoRe, using p53 core co-ordinates.

<sup>b</sup>p53–Bp1 complex from AMoRe, using p53 and Bp1 co-ordinates.

$R_{\text{sym}} = \sum_h \sum_l |I_{h,l} - \langle I_h \rangle| / \sum_h \sum_l I_{h,l}$  where  $\langle I_h \rangle$  is the mean intensity of the *i*th observation of the reflection *h*.

$R\text{-factor} = \sum |F_{\text{obs}}| - |F_{\text{calc}}| / \sum |F_{\text{obs}}|$ .

*R*<sub>free</sub> is calculated from data excluded from refinement.

*G*-factor is the overall measure of structure quality from Procheck (Laskowski *et al.*, 1993).

R.m.s.ds, root mean square deviations.

expressed in *Escherichia coli* and purified to homogeneity. We incubated the proteins with the recombinantly expressed DNA-binding domain of p53 (residues 96–308) and analysed the resulting complexes by gel filtration (Derbyshire *et al.*, 2002). The region comprising residues 1722–1971 was found to form a stable complex with p53 suitable for crystallographic investigation. This region encompasses both predicted BRCT domains. The p53–BP1 complex has been crystallized and its three-dimensional structure determined, in part, by molecular replacement from the co-ordinates of the p53 core domain (Cho *et al.*, 1994). Finally, the structure determination was completed by using a molecular replacement solution obtained using the co-ordinates of the p53–BP1 complex as a search model (PDB ID, 1KZY; Joo *et al.*, 2002) and refined at 2.6 Å resolution (Table I; PDB ID, 1GZH).

### Overall structure of the complex

Crystals of the complex display orthorhombic symmetry with two heterodimers (I and II) of p53 in complex with the C-terminal region of 53BP1(BP1) in the asymmetric unit (Figure 1). The heterodimers predominantly pack together via contacts between the N-terminal BRCT domains. There are few molecular contacts between the p53 domains despite their proximity to one another. Overall, clear electron density was interpretable throughout the structures of both p53–BP1 heterodimers, with

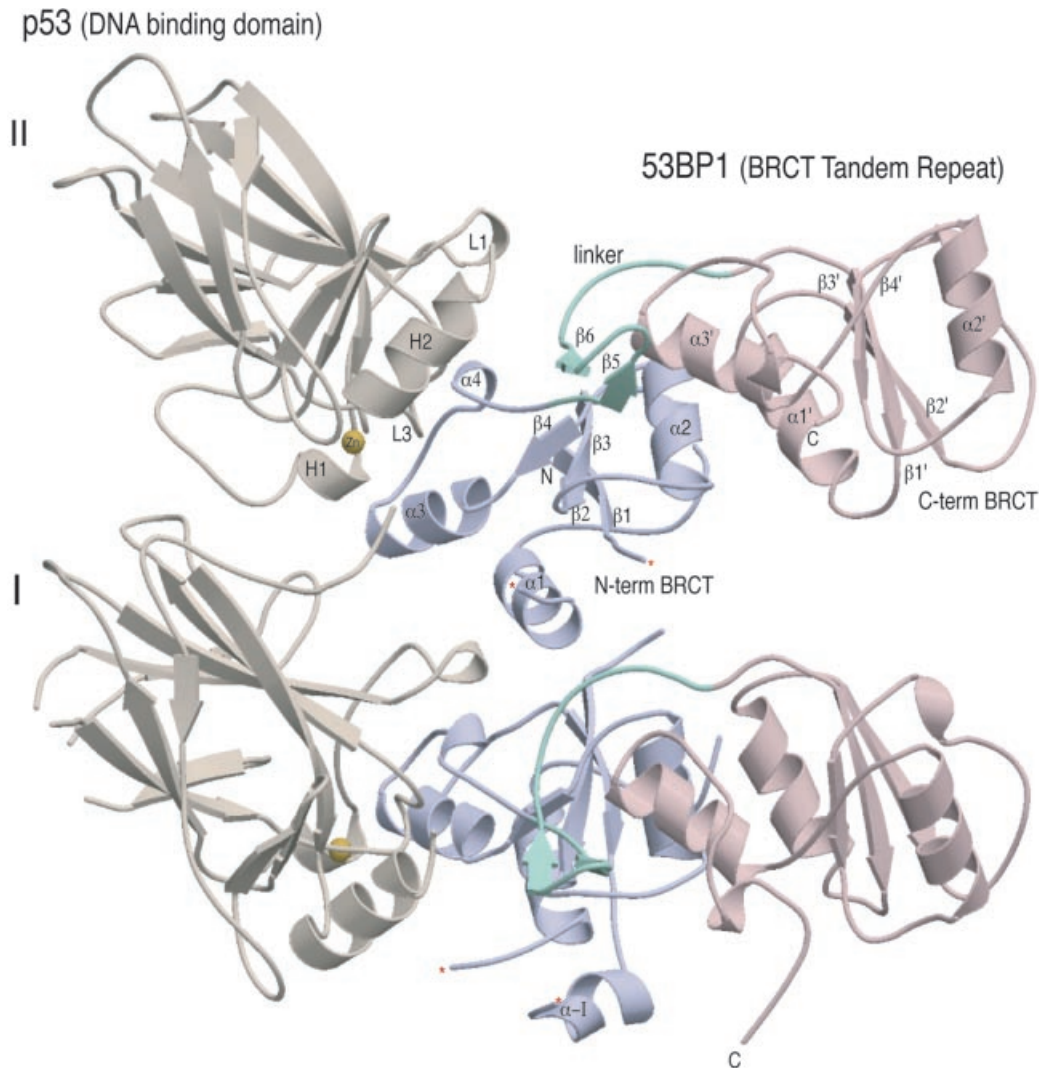


**Fig. 1.** Crystal structure of the 53BP1–p53 complex. Structure of the asymmetric unit containing four molecules, two heterodimers (I and II) of p53 DNA-binding domain (brown) in complex with the BRCT tandem repeat of 53BP1 (blue and pink). The heterodimers pack together mainly through contacts made between the N-terminal region of 53BP1. There are no contacts made between the adjacent p53 molecules. The single zinc atom bound to p53 is shown in yellow and the 53BP1 inter-domain linker is shown in green. ‘Missing’ residues in the structure are denoted by an asterisk.

slight variations in the structure of the loop regions involved in close crystal contacts. The first molecule of p53 extends from residue S95 to K292 with breaks in the electron density between residues 183–188 and 224–227, and at residue 200. The second copy of p53 has no such breaks, but only stretches from S95 to L289. Electron density for the first copy of BP1 was interpretable from L1724 to S1971, and in the second BP1 molecule from N1725 to Y1969. With the exception of breaks between residues 1793–1798 (first copy) and 1794–1796 (second copy), the only region of the binding protein not clearly visible in our structure corresponds to a unique insertion found in BP1 between residues 1740 and 1768, although there is some limited density for residues 1741–1750 ( $\alpha$ -I) in the first copy of BP1 (Figure 1).

The structure of the heterodimer reveals that the DNA-binding domain of p53 interacts specifically with the N-terminal BRCT domain of 53BP1 (Figure 1). The overall morphology of the complex is roughly L-shaped (~60 Å long in both directions and ~30 Å in thickness),

with p53 binding to a structural motif extending from  $\alpha$ 3 of the N-terminal BRCT domain and including the linker region that extends between the two BRCT domains. The C-terminal BRCT domain extends away from the p53 interaction surface. The overall fold of the 53BP1 BRCT tandem repeat is similar to the BRCT domains of human BRCA1 (Figure 2A). The fold of the BRCT domains is characterized by a central four-stranded  $\beta$ -sheet, with a pair of  $\alpha$ -helices ( $\alpha$ 1 and  $\alpha$ 3) packed against one face and a single helix ( $\alpha$ 2) packed against the opposite face of the sheet (Figure 2A). The  $\beta$ -sheet forms the core of the structure, with helix  $\alpha$ 1 forming hydrophobic interactions with residues from  $\beta$ 1 and  $\beta$ 2. Helix 2 ( $\alpha$ 2) interacts with  $\beta$ 4, also through hydrophobic interactions (Figure 2B). This is further stabilized by hydrogen bonding, curiously only in the N-terminal domain, between the base of  $\alpha$ 2 to the  $\alpha$ 2/ $\beta$ 4 loop (R1813 and D1790) (Figure 2B). In the N-terminal domain,  $\alpha$ 1 and  $\alpha$ 3 form a two-helical bundle, solely through hydrophobic interactions. Helix 3 ( $\alpha$ 3) contains the highly conserved tryptophan residue, which

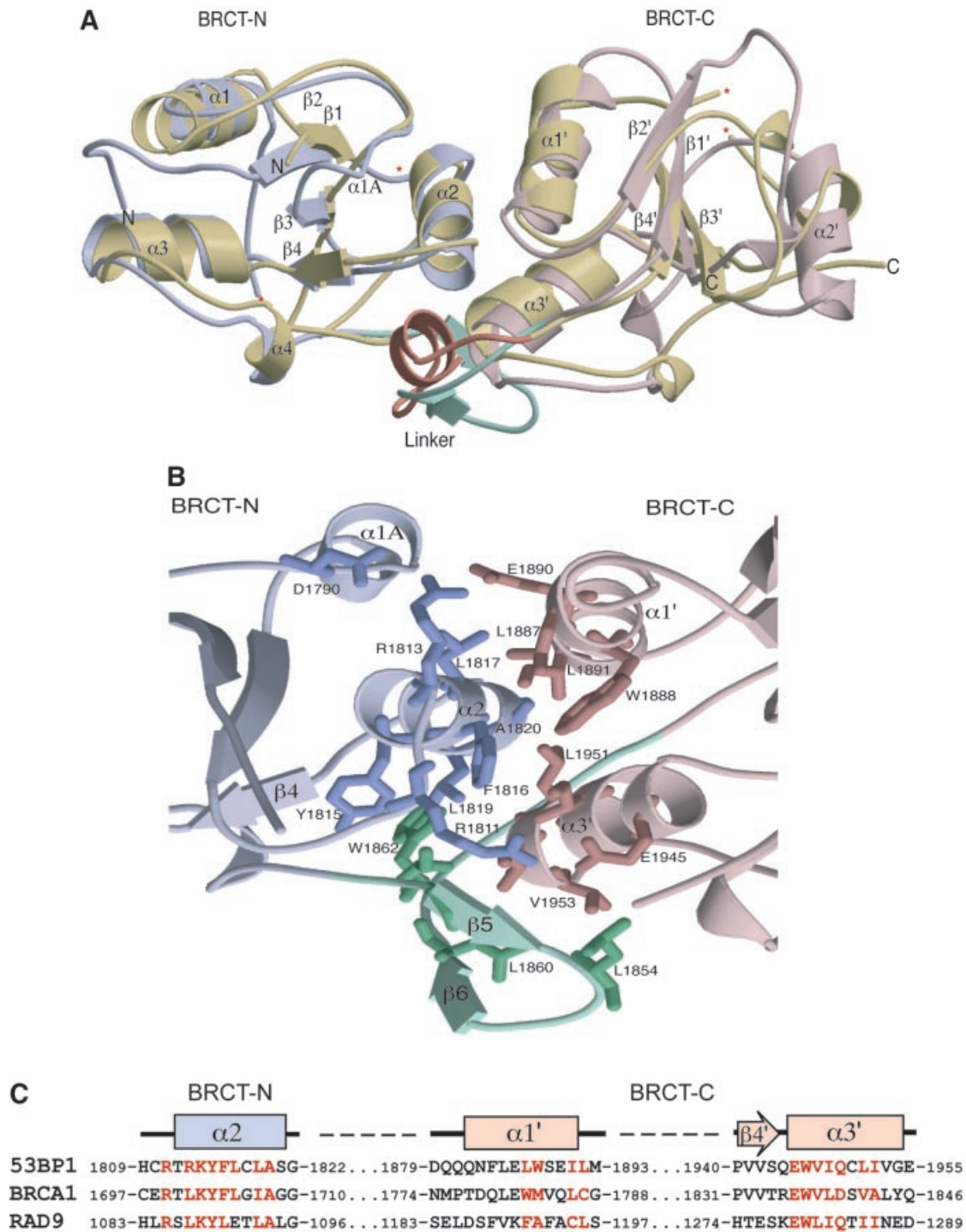


**Fig. 2.** Structural features of the 53BP1 tandem BRCT repeat. (A) A secondary structure representation of the superimposition of the BRCT tandem repeats from human BRCA1 and 53BP1. The N- and C-terminal BRCT domains of 53BP1 are coloured in light blue and pink, respectively, whilst both BRCT domains of human BRCA1 are coloured gold. The linker regions of each tandem repeat are also highlighted; BRCA1 (a loop-helix-loop structure) in orange and 53BP1 (a  $\beta$ -ribbon-like motif) in green. 'Missing' residues in the structure are denoted by an asterisk. (B) Intra-molecular interactions at the inter-BRCT repeat interface of 53BP1. The side chains from the first BRCT repeat are shown in blue, those from the linker are in pink and those from the second BRCT repeat are green. The  $\alpha 2$  helix of the first repeat together with  $\alpha 1'$  and  $\alpha 3'$  helices of the second repeat form a three-helical bundle that is stabilized by  $\alpha 1A$  and the  $\beta$ -hairpin linker ( $\beta 5$ - $\beta 6$ ). (C) An amino acid sequence alignment of the regions of BRCA1, 53BP1 and RAD9 that are predicted to form BRCT-BRCT interfaces. Residues that constitute this interface in human 53BP1, as well as conserved residues in human BRCA1 and *Saccharomyces cerevisiae* RAD9, are coloured red.

interacts with other conserved 'core' residues from  $\beta 1$ ,  $\beta 3$  and  $\beta 4$  as well as the segment involved in p53 binding (Figure 2B).

The 53BP1 inter-BRCT repeat interface contains both core BRCT structural elements and also the inter-domain linker (Figure 2B). The interface buries  $\sim 2500 \text{ \AA}^2$  of

surface area, with one third of this area contributed by the inter-domain linker. The  $\alpha 1'$  and  $\alpha 3'$  helices pack against  $\alpha 2$ , forming a three-helical bundle structure. The interface is stabilized by hydrophobic residues contributed by the bundle, with extra stability being provided by two arginine residues; R1813 at the base of  $\alpha 2$ , which interacts directly with E1890 on  $\alpha 1'$  and D1790 on  $\alpha 1A$ , and R1811, which forms a salt bridge with E1945 of  $\alpha 3'$  (Figure 2B). The inter-domain linker adopts a  $\beta$ -hairpin structure ( $\beta 5$ – $\beta 6$ ; residues 1851–1860) followed by an extended structure (residues 1861–1867). The linker packs extensively with both BRCT repeats at the inter-BRCT interface (Figure 2B). This packing is stabilized by hydrophobic residues from one face of the  $\beta$ -hairpin structure that stacks against residues from the  $\alpha 2$  and  $\alpha 3'$  helices of the three-helical bundle.

The structure of the p53 core domain in this complex is similar to the crystal structures of free and DNA-bound forms of p53 (Figure 1; Cho *et al.*, 1994). p53 domain consists of a  $\beta$ -sandwich with a 'greek key' topology that serves as a scaffold for two large loops, L2 (163–195) and L3 (236–251), and a loop-sheet-helix motif, H2 (278–286). The two loops bind a single zinc atom, which is tetrahedrally co-ordinated by C176 and H179 of L2, and C238 and C242 of L3 (Figure 1). This region, together with the H2 helix, forms a continuous surface at one end of the  $\beta$ -sandwich, which is known to be critical for p53's function and its inactivation in tumours. This area is one of the most conserved regions of p53 to which most of the tumorigenic mutations map (Cho *et al.*, 1994). Interestingly, this conserved region of p53 represents the sole 53BP1-binding interface. In this complex,  $\sim 1400$  Å<sup>2</sup> of mostly polar surface area is buried in the p53–BP1 interface. In the BP1–p53 complex, the C-terminal portion of the first BRCT repeat and the linker region of 53BP1 forms a continuous surface that binds part of the DNA-binding surface of the p53 core domain, mostly through contacts to the L3 loop, but a smaller number of contacts are made via the L2 loop (Figure 1). A surprising feature of the complex is that the C-terminal BRCT domain of 53BP1 is positioned distantly from the p53 molecule and makes no contacts with the core domain (Figure 1). The significance of this architecture will be discussed later.

#### Comparison of 53BP1 with other BRCT structures

The overall structure of the individual 53BP1 BRCT domains is similar to that observed in the C-terminal repeat of BRCA1 (Figure 2; Williams *et al.*, 2001), as well as in the individual BRCT domains of XRCC1 and ligase III (Zhang *et al.*, 1998; Krishnan *et al.*, 2001). A structural alignment of the BRCT repeats of 53BP1 with the BRCA1, XRCC1 and ligase III BRCT domains reveals that the relative arrangement of the central  $\beta$ -sheet and helices ( $\alpha 1$  and  $\alpha 3$ ) is conserved in all the four repeats (data not shown). However, the conformations of the  $\beta 1$ – $\alpha 1$ ,  $\beta 2$ – $\beta 3$  and  $\beta 3$ – $\alpha 2$  connecting loops, as well as the orientation of  $\alpha 2$  relative to the central  $\beta$ -sheet, are much less conserved. The conservation of the  $\alpha 1$ – $\alpha 3$ – $\beta$ -sheet structure is maintained by the packing of a limited number of key conserved hydrophobic residues in the core of the BRCT fold. The structure of the 53BP1 BRCT region closely resembles that of human BRCA1, especially in the

N-terminal domain. However, the structures of the C-terminal BRCTs are considerably different. BRCA1 lacks the  $\alpha 2'$  helix, which in p53BP1 is presented on the surface of this BRCT domain. Furthermore, the adjacent loop ( $\beta 2'$ – $\alpha 3'$ ) has a different conformation between these two proteins. The N-terminal BRCT domain of BP1 contains a unique large insertion of 29 residues (1741–1769) rich in polar and charged residues between  $\beta 1$  and  $\alpha 1$  that are not found in BRCA1 or other BRCTs. In our structure, this region is very disordered, probably indicating that it is highly flexible. However, in the first copy of BP1, some broken electron density is interpretable for residues 1741–1750 and there is good indication from model building that these residues form an  $\alpha$ -helical structure ( $\alpha$ -I) that extends from the surface of the N-terminal BRCT domain into the solvent (Figure 1).

The entire tandem BRCT structures of 53BP1 and BRCA1 can be superimposed with a root mean square deviation (r.m.s.d.) of 6.27 Å (Figure 2A). This value improves to 1.85 Å when matching only 135 C $\alpha$  positions, including all the central  $\beta$ -strands and  $\alpha$ -helices (Figure 2A). The most notable structural conservation between these two structures exists at the inter-BRCT repeat interface. As discussed above, two inter-BRCT repeats of 53BP1 interact through intramolecular head-to-tail contacts, burying a large amount of surface area in this interface (Figure 2B). The core of this interface is formed by the interaction of three  $\alpha$ -helices:  $\alpha 2$  of the N-terminal repeat, and  $\alpha 1'$  and  $\alpha 3'$  from the C-terminal repeat (Figure 2B). The residues in these helices that contribute to the interface are almost all hydrophobic and pack tightly in a knobs-in-holes manner. In the crystal structure of human BRCA1, the two inter-BRCT repeats also pack via a triple helical interface similar to that seen in the 53BP1 structure (Williams *et al.*, 2001; Figure 2B). Multiple BRCT repeats are common in many of the BRCT-containing proteins such as BRCA1, RAD9 and DNA ligase IV. An amino acid sequence alignment of the two 53BP1 BRCT repeats with those in BRCA1 and Rad9 shows that the residues occupying the interface between the two repeats in  $\alpha 2$ ,  $\alpha 1'$  and  $\alpha 3'$  of 53BP1 are highly conserved in BRCA1 (Figure 2C; Williams *et al.*, 2001), and it is likely that this mode of intra-molecular packing will be common within the repeats of the BRCT family. The inter-repeat linker of 53BP1 occupies a similar position as that of human BRCA1, packing on one side of the three-helical bundle and stabilizing the inter-BRCT repeat interface (Figure 2B). There is continuous electron density for the linker connecting the two BP1 BRCTs. In contrast, the structure of the linker connecting the human BRCA1 BRCT repeats is poorly ordered, possibly indicating flexibility. The central portion of the BRCA1 linker, however, is clearly  $\alpha$ -helical. In the BP1 linker, this region forms a distinct  $\beta$ -ribbon structure ( $\beta 5$ – $\beta 6$ ; Figure 2B).

Many BRCT domains have been shown to interact with specific partners through either homo (e.g. Rad9) or hetero (e.g. XRCC1–ligase III) BRCT–BRCT interactions (Huyton *et al.*, 2000). In our crystals, we noted that the N-terminal BRCT domains from neighbouring 53BP1 molecules in the unit cell form non-crystallographic interactions. The interface is composed of interactions between  $\alpha 1'$  and an extended loop region between  $\beta 1$  and

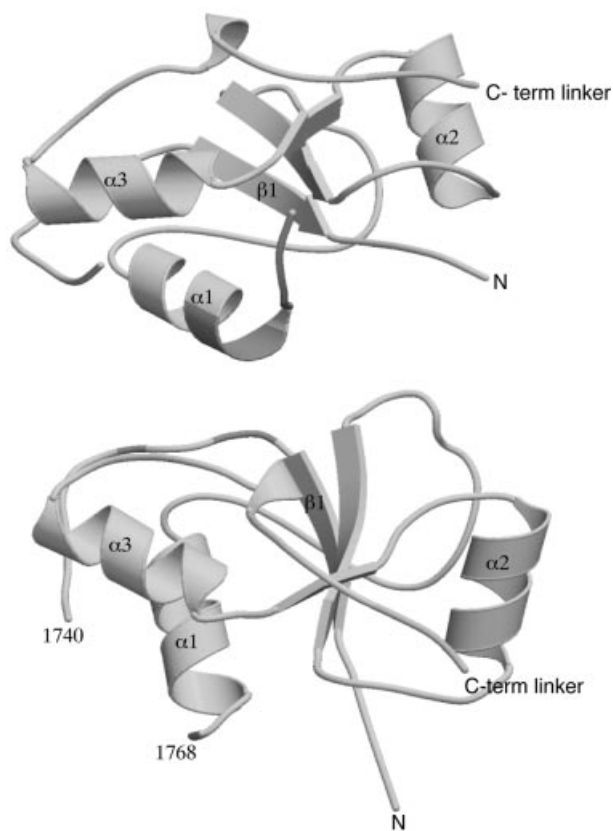


**Fig. 3.** Contacts between 53BP1 BRCT–BRCT domains. The N-terminal BRCT domains form non-crystallographic interactions. The interface is composed of non-specific interactions between residues in  $\alpha 1$  and an extended loop region, shown in shaded colour.

$\alpha 1$  (Figure 3). A closer examination of this interface showed that there are no hydrogen bonds or electrostatic contacts, suggesting that this interaction is unlikely to represent a specific BRCT–BRCT interface.

#### **Structure of the 53BP1–p53 interface**

A striking feature of the complex is that 53BP1 interacts with p53 through a very limited number of specific contacts localized around the inter-domain linker. The p53-binding region of 53BP1 forms an unusual extended structure, which extends from the C-terminal region of the first BRCT ( $\alpha 3$  helix) into the central helical region ( $\alpha 4$ ) of the inter-domain linker (approximately residues 1843–1867). The linker, a  $\beta$ -ribbon structure ( $\beta 5$ – $\beta 6$ ; Figure 4A), then proceeds into the next domain as strand  $\beta 1'$  in a fashion not dissimilar to the extended region leading into  $\beta 1$  of the N-terminal domain. This may represent a BRCT–BRCT linkage more suited to multiple BRCT repeats. Interestingly, this linker region is distinct from that of the human BRCA1 tandem repeat, which forms a loop–helix–loop structure (Figure 2A). All the 53BP1 contacts are with highly conserved residues on the L2 and L3 loops of p53. The L2 and L3 loops form rigid hairpin structures stabilized by a single co-ordinating zinc atom and also by multiple intra-molecular hydrogen bonds. The COOH-terminal of the L3 hairpin (247–249) is juxtaposed to the extended linker region at the C-terminal region of the first BRCT of 53BP1

(Figure 4A). Arg 248 from this loop hydrogen bonds with Asp 1861 from the  $\beta$ -hairpin of the inter-repeat linker and also hydrogen bonds to the backbone carbonyl group of Leu 1847 at the beginning of the linker (Figure 4B). The conformation of this arginine residue is stabilized by stacking interaction with the ring of Pro 1849 (Figure 4B). Asn 247 also forms a main-chain hydrogen bond with Leu 1847, and Arg 249 hydrogen bonds with Arg 1844 and Asn 1845 from  $\alpha 4$  (Figure 4B). The Met 243 side-chain of p53 makes van der Waals contacts with Val 1829 and Tyr 1846 (Figure 4B). The L2 loop (163–195) of p53 also makes major contributions to the 53BP1-binding surface (Figure 4A). Arg 181 forms a charge-stabilized hydrogen bond with Asp 1833 and also forms a stacking interaction with the aromatic ring of His 1836 (Figure 4B). Glu 177 hydrogen bonds to Asn 1842 and additional hydrogen bonds are also made in the complex (Gln 165–Asp 1861, Gln 167–Gln 1863, Glu 171–Asn 1842).

#### **Effects of site-specific and tumorigenic p53 mutations**

It has been reported that the binding of 53BP1 to p53 inhibits binding to DNA and 53BP2 *in vitro* (Iwabuchi *et al.*, 1994). Our structure reveals the molecular basis for this inhibition. The p53-binding site of 53BP1 directly overlaps with the DNA- and 53BP2-binding sites, and therefore sterically blocks the docking of these ligands (Figure 4A; Cho *et al.*, 1994; Gorina and Pavletich, 1996). More specifically, a comparison of the 53BP1–p53 structure with both the p53–DNA and p53–53BP2 complexes showed that many common residues, including those on the highly conserved loops L2 and L3, provide many of the important contacts in these complexes. Alanine scanning mutagenesis has confirmed this and has shown that a number of these conserved residues are involved in the binding of all three ligands (Thukral *et al.*, 1994). The significance of many of these conserved interactions is highlighted by the residue Arg 248 (Figure 4B). *In vivo*, this residue is the most frequently mutated amino acid of p53. The replacement of this residue by alanine abolishes 53BP1, DNA and 53BP2 binding, confirming its pivotal role in p53 ligand interactions (Figure 4B; Thukral *et al.*, 1994). The failure of many tumour-derived p53 mutants to bind to 53BP1 also closely correlates with their failure to bind to DNA or 53BP2. This is not unexpected, since we have demonstrated that the 53BP1-, DNA- and 53BP2-binding surfaces all appear to overlap considerably. Is it possible that the disruption of 53BP1 binding by tumorigenic mutations may be secondary to their disruption of DNA binding, and the loss of 53BP1 binding may have no functional consequence for tumorigenesis? Pavletich and colleagues noted previously that among the p53 surface residues with no apparent structure-stabilizing roles, those that contact either 53BP1 or 53BP2 but not DNA (Gorina and Pavletich, 1996) are also found mutated, although at lower frequencies and, conversely, residues that contact only the DNA but not 53BP1 or 53BP2 also show similarly low mutational frequencies. However, the highest mutational frequencies occur at residues involved in 53BP1, DNA and 53BP2 binding (e.g. Arg 248). It is also notable that Met 243, an important 53BP1 contact but has no

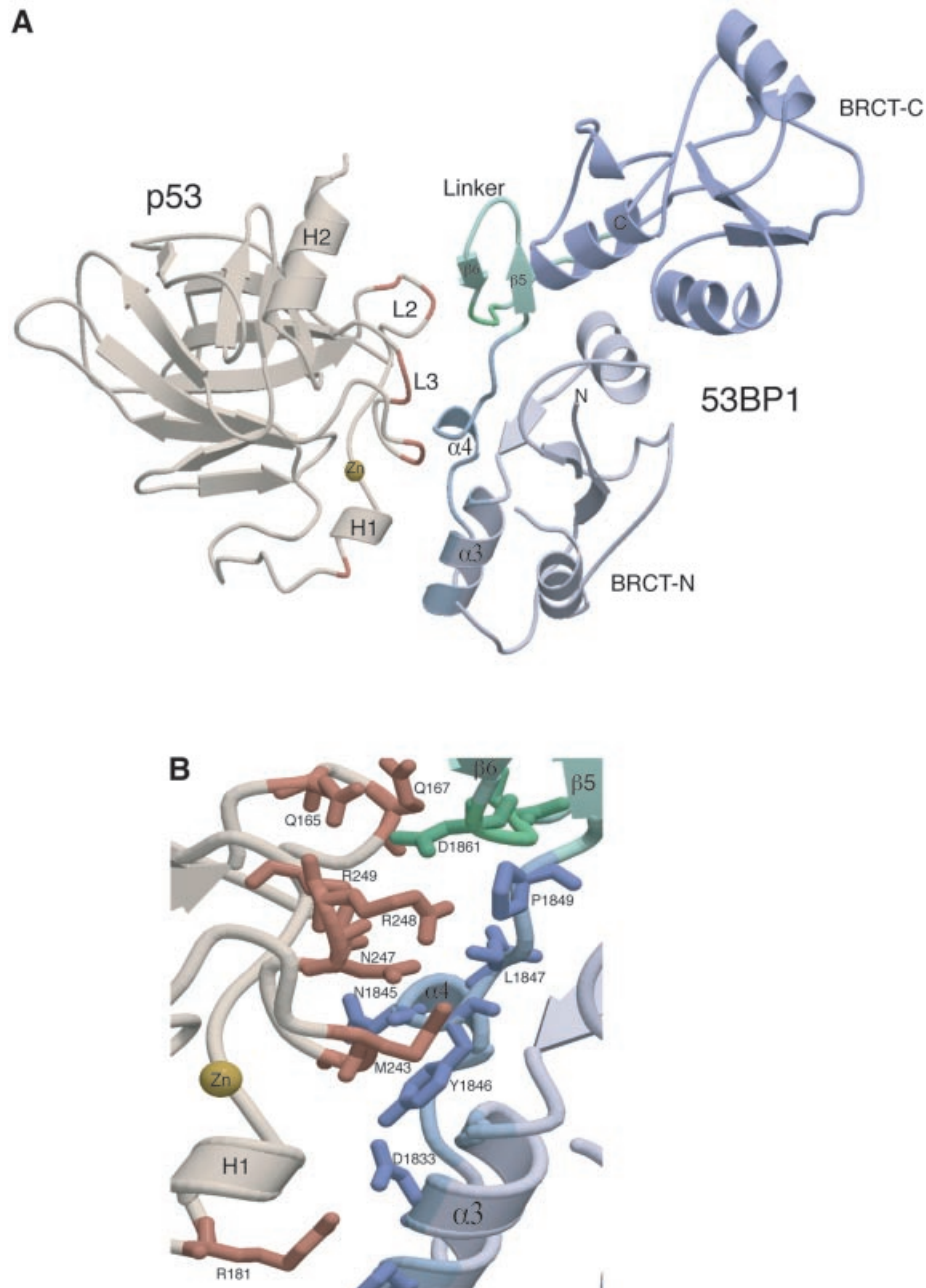


**Fig. 4.** Structure of the 53BP1-p53 interface. (A) The heterodimeric complex of 53BP1 bound to p53. The p53 binding region of 53BP1 forms an extended structure from the N-terminal region of the first BRCT (shown in light blue) to the central helical region of the inter-domain linker ( $\alpha 4$ ). The 53BP1 contacts (shown in brown) are with highly conserved residues on the L2 and L3 loops of p53. The L2 and L3 loops form rigid hairpin structures that are stabilized by a single co-ordinating zinc atom (yellow). (B) Specific amino acid contacts at the complex interface between 53BP1 (blue) and p53 (brown). The inter-domain  $\beta$ -turn ( $\beta 5$ - $\beta 6$ ) is shown in green.

apparent role in structure stabilization or DNA recognition, is also mutated in cancer.

#### **A conserved protein-protein binding motif in BRCT domains**

It is now evident that BRCT domains physically mediate interactions between different proteins (Huyton *et al.*, 2000), suggesting that one specific role for these domains is to promote specific protein-protein interactions *in vivo*. The importance of the inter-BRCT linker in mediating protein-protein interactions was first highlighted by biochemical studies (Grawunder *et al.*, 1998; Taylor *et al.*,

1998) and subsequently supported by the structure of the XRCC4-ligase IV linker complex (Sibanda *et al.*, 2001). A notable feature of the 53BP1-p53 complex is also the very localized nature of the interactions, around the linker, between the BP1 BRCTs and p53. We examined the local structure of BP1 at the BRCT-p53 interface and compared this with the uncomplexed BRCT domains of BRCA1, XRCC1 and ligase III. Figure 5 shows a superimposition of the p53-binding interface of BP1 with the equivalent regions of BRCA1 and XRCC1. The  $C_{\alpha}$  backbone of these regions overlap with an r.m.s.d. of  $<1$  Å, confirming that they form almost identical structural motifs. This structure

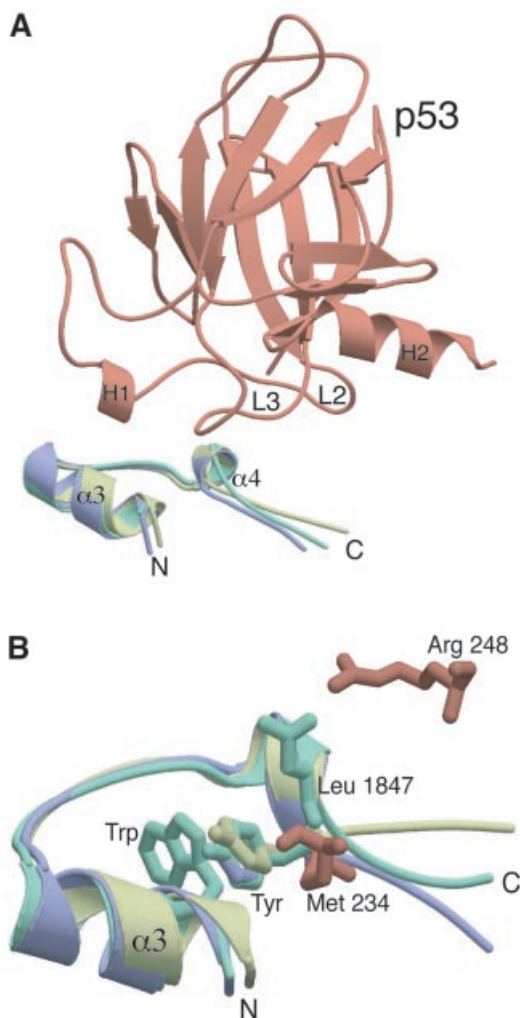


**Fig. 5.** A conserved protein binding motif in BRCT domains. (A) Superimposition of the conserved p53-binding motif. This shows a superimposition of the p53-binding interface of 53BP1 (green; residues 1829–1849) with the comparable regions of the BRCT domains of BRCA1 (blue; 1716–1738) and XRCC1 (yellow; 72–94). The  $C_{\alpha}$  backbone of these regions overlap with an r.m.s.d. of  $<1$  Å. The position of this motif in relation to p53 binding is also shown (p53 core domain is shown in brown). (B) The highly conserved Trp residue on  $\alpha 3$  is positioned in an identical position in all three structures (for clarity only a single Trp is shown) and stacks against the conserved Tyr residue (the superimposed Tyr shown). Two conserved 53BP1–p53 interactions are shown, Arg 248–Leu 1847 and Met 243–Tyr 1846.

has a highly conserved helix ( $\alpha 3$ )–loop–helix ( $\alpha 4$ )–loop conformation in all three structures (Figure 5A). Does this structural conservation also reflect a conserved functional role for this motif? In the 53BP1–p53 complex, the majority of the contacts are made with residues in the short  $\alpha$  helix ( $\alpha 4$ ; NYRNYLL, residues 1842–1848). In the BRCA1 and XRCC1 BRCT domains, many of these residues are also highly conserved (N-x-H/R-N/D-Y/F-x-L/V). The position of the side chains of these conserved Asn, Asn/Asp and Tyr/Phe are absolutely conserved in the short helix ( $\alpha 4$ ) and, more importantly, these residues make important interactions with p53 (Figure 5B). Tyr 1846 makes van der Waals contact with Met 243, Asn 1842 hydrogen bonds to Glu 177 and Asn 1845 hydrogen

bonds with Arg 249. Based on these findings, it seems likely that this conserved ‘BRCT recognition motif’ may be important for the binding of target proteins by BRCT domains. We also noted that the highly conserved tryptophan residue (Trp 1830 in BP1), found in most BRCT domains on  $\alpha 3$ , is positioned in an identical position in all three structures (Figure 5B). This tryptophan residue stacks tightly against the conserved tyrosine residue (Tyr 1846 in BP1) in all the BRCT structures (Figure 5B), suggesting that this conserved interaction may be important for stabilizing the conformation of the conserved BRCT recognition motif.

### Conclusions

Since it was first reported that the breast cancer susceptibility gene contained two copies of a conserved BRCT domain at its C-terminus, and found subsequently in a variety of proteins involved in DNA repair, recombination and cell-cycle control, there has been a lot of speculation about the physiological role of this highly conserved structural motif. Recent biochemical data has indicated that the BRCT domain functions as a protein–protein interaction module. In this report, we describe the crystal structure of a tandem repeat of BRCT domains (53BP1) in complex with an intra-cellular target protein (p53) allowing us to directly visualize the molecular contacts in a BRCT–protein complex. The structure of this complex highlights the importance of the BRCT inter-domain linker and interface in protein–protein interactions. The  $\alpha 4$  helix of the N-terminal BRCT domain and the inter-domain linker region form what we have termed the ‘BRCT recognition motif’. This recognition motif stacks against the inter-repeat interface, which is highly conserved in other tandem BRCT repeats, including BRCA1. This structural motif is responsible for all the major interactions with p53 and is conserved in the structures of other BRCT domains, probably reflecting a conserved functional role in protein recognition. BRCT domains are often found in pairs (Bork *et al.*, 1997; Callebaut and Mornon, 1997), and it is probable that the conserved interface between BRCT tandem repeats is required to stabilize and present the correct conformation of the recognition motif, allowing this region to bind to protein partners. This mode of binding may represent only one of many distinct modes of protein recognition utilized by BRCT domains. Strikingly, in the 53BP1–p53 complex, the position of the C-terminal BRCT domain is distant from the p53-binding site and, consequently, it plays no role in p53 binding. It is tempting to speculate that BRCTs may also interact with other ligands via contacts with the central globular core of the BRCT motif. This promiscuity would allow BRCTs, such as the C-terminal BRCT of BP1, to simultaneously mediate interactions with multiple protein partners. However, we must first elucidate the structures of many more BRCT–protein complexes before we can delineate the determinants that specify the full range of BRCT–protein interactions.

After submission of this manuscript, the structure of the 53BP1 BRCT region bound to p53 was reported (Joo *et al.*, 2002). This structure is in good agreement with the findings reported in this paper.



## Materials and methods

### Purification and crystallization of the p53–53BP1 complex

p53 (residues 94–312) and 53BP1 (residues 1722–1972) were over-expressed separately in the *E. coli* strain B834(DE3) plysS (Novagen) as described previously (Derbyshire *et al.*, 2002). The p53 DNA-binding domain was purified by SP and heparin–Sepharose column chromatography. The 53BP1 BRCT tandem repeat protein was purified by Ni-NTA agarose and Hi-Trap Q Sepharose column chromatography (Derbyshire *et al.*, 2002). The p53–BP1 complex was formed by dialysis and the heterodimer purified by size exclusion chromatography using a preparative Superdex-75 column. For optimal crystallization, the p53–BP1 complex was concentrated to ~15 mg/ml. Crystals were grown by the micro-batch technique under mineral oil by mixing protein with an equal volume of a precipitant solution containing 50 mM Tris–HCl pH 7.4, NH<sub>3</sub>SO<sub>4</sub> and 20–25% polyethylene glycol 4 kDa (PEG 4k; Derbyshire *et al.*, 2002).

### Structure determination

A native data set was measured to a resolution of 2.6 Å from a crystal of the complex cooled to 100 K. Indexing was performed using the MOSFLM software (Leslie, 1992). The data were scaled and reduced using the CCP4 suite (CCP4, 1994). Initial work on the structure of the p53–BP1 complex proceeded via a partial molecular replacement solution obtained using the co-ordinates of the DNA-binding domain of p53 alone. Two p53 molecules were found in the asymmetric unit by molecular replacement using AMoRe (Navaza, 1994) and the co-ordinates of the p53 DNA-binding domain (PDB ID, 1TSR; Cho *et al.*, 1994). Through the use of multi-domain non-crystallographic symmetry averaging (DM in CCP4, 1994), as well as cross-crystal averaging (DMulti in CCP4, 1994), both being combined with solvent flattening and extensive phase extension, a gradual improvement in electron density quality and interpretability was observed (Derbyshire *et al.*, 2002). Finally, the structure was completed using a molecular replacement solution obtained using the co-ordinates of the p53–BP1 complex (PDB ID, 1KZY; Joo *et al.*, 2002). Rigid body refinement by Refmac (CCP4, 1994) was conducted with four independent bodies, two molecules each of p53 and BP1, giving a final correlation coefficient of 47.6%. Once again, density modification procedures were adopted to improve the electron density prior to molecular modelling. Model building with the Xfit program of XTALVIEW (McRee, 1999) was alternated with crystallographic refinement using CNS (Brünger *et al.*, 1998). After the addition of 110 water molecules and two SO<sub>4</sub> ions, the crystallographic *R*-factor and *R*<sub>free</sub> factor were 23.81 and 28.83, respectively. The stereochemistry of the structure was assessed with PROCHECK (Laskowski *et al.*, 1993) and 100% of the residues were in the favourable regions of the Ramachandran plot. Details and statistics of the final refined model are presented in Table I. The atomic co-ordinates have been deposited in the Protein Data Bank (PDB ID, 1GZH). Figures were generated with several combined uses of MOLSCRIPT (Kraulis, 1991) and Raster3D (Merritt and Bacon, 1997).

## Acknowledgements

We are indebted to Dr N.Pavletich for providing co-ordinates of the p53–53BP1 complex prior to publication. We would like to thank Professor R.Read and Drs R.Pannu, Y.Müller, G.Spraggon and M.Noble for invaluable crystallographic advice. We would also like to thank Drs L.Itzhaki, F.Rousseau and J.Schymkowitz for their support in the early stages of this work. A.J.D. is Royal Society University Research Fellow, and work in the A.J.D. laboratory is supported by grants from Cancer Research UK, Leukaemia Research Fund, BBSRC, the Association for International Cancer Research and the Royal Society. K.I. is supported by project research grants (H99-1, H00-1 and H01-1) from the High-Technology Center of Kanazawa Medical University, Japan.

## References

Anderson,L., Henderson,C. and Adachi,Y. (2001) Phosphorylation and rapid relocalization of 53BP1 to nuclear foci upon DNA damage. *Mol. Cell. Biol.*, **21**, 1719–1729.

Bargonetti,J., Manfredi,J.J., Chen,X., Marshak,D.R. and Prives,C. (1993) A proteolytic fragment from the central region of p53 has marked sequence-specific DNA-binding activity when generated

from wild-type but not from oncogenic mutant p53 protein. *Genes Dev.*, **7**, 2565–2574.

Bork,P., Hofmann,K., Bucher,P., Neuwald,A.F., Altschul,S.F. and Koonin,E.V. (1997) A superfamily of conserved domains in DNA damage-responsive cell cycle checkpoint proteins. *FASEB J.*, **11**, 68–76.

Brünger,A.T. *et al.* (1998) Crystallography and NMR system: a new software suite for macromolecular structure determination. *Acta Crystallogr. D Biol. Crystallogr.*, **54**, 905–921.

Callebaut,I. and Mornon,J.P. (1997) From BRCA1 to RAP1: a widespread BRCT module closely associated with DNA repair. *FEBS Lett.*, **400**, 25–30.

CCP4 (1994) The CCP4 suite: programs for protein crystallography. *Acta Crystallogr. D Biol. Crystallogr.*, **50**, 760–763.

Chai,Y.L., Cui,J., Shao,N., Shyam,E., Reddy,P. and Rao,V.N. (1999) The second BRCT domain of BRCA1 proteins interacts with p53 and stimulates transcription from the p21WAF1/CIP1 promoter. *Oncogene*, **18**, 263–268.

Chapman,M.S. and Verma,I.M. (1996) Transcriptional activation by BRCA1. *Nature*, **382**, 678–679.

Cho,Y.J., Gorina,S., Jeffrey,P.D. and Pavletich,N.P. (1994) Crystal structure of a p53 tumor suppressor–DNA complex: understanding tumorigenic mutations. *Science*, **265**, 346–355.

Critchlow,S.E., Bowater,R.P. and Jackson,S.P. (1997) Mammalian DNA double-strand break repair protein XRCC4 interacts with DNA ligase IV. *Curr. Biol.*, **7**, 588–598.

Derbyshire,D.J., Basu,B.P., Iwabuchi,K. and Doherty,A.J. (2002) Purification, crystallization and preliminary X-ray analysis of a complex of the BRCT domains of human 53BP1 bound to the p53 tumour suppressor. *Acta Crystallogr. D Biol. Crystallogr.*, in press.

Gorina,S. and Pavletich,N.P. (1996) Structure of the p53 tumor suppressor bound to the ankyrin and SH3 domains of 53BP2. *Science*, **274**, 1001–1005.

Grawunder,U., Wilm,M., Wu,X., Kulesza,P., Wilson,T.E., Mann,M. and Lieber,M.R. (1997) Activity of DNA ligase IV stimulated by complex formation with XRCC4 protein in mammalian cells. *Nature*, **388**, 492–495.

Grawunder,U., Zimmer,D. and Lieber,M.R. (1998) DNA ligase IV binds to XRCC4 via a motif located between rather than within its BRCT domains. *Curr. Biol.*, **8**, 873–876.

Hollstein,M., Sidransky,D., Vogelstein,B. and Harris,C.C. (1991) p53 mutations in human cancers. *Science*, **253**, 49–53.

Horikoshi,N., Usheva,A., Chen,J.D., Levine,A.J., Weinmann,R. and Shenk,T. (1995) Two domains of p53 interact with the TATA-binding protein and the adenovirus 13S E1A protein disrupts the association, relieving p53-mediated transcriptional repression. *Mol. Cell. Biol.*, **15**, 227–234.

Huyton,T., Bates,P.A., Zhang,X., Sternberg,M.J. and Freemont,P.S. (2000) The BRCA1 C-terminal domain: structure and function. *Mutat. Res.*, **460**, 319–332.

Iwabuchi,K., Bartel,P.L., Li,B., Marraccino,R. and Fields,S. (1994) Two cellular proteins that bind to wild-type but not mutant p53. *Proc. Natl Acad. Sci. USA.*, **91**, 6098–6102.

Iwabuchi,K., Li,B., Massa,H.F., Trask,B.J., Date,T. and Fields,S. (1998) Stimulation of p53-mediated transcriptional activation by the p53-binding proteins, 53BP1 and 53BP2. *J. Biol. Chem.*, **273**, 26061–26068.

Joo,W.S., Jeffrey,P.D., Cantor,S.B., Finnin,M.S., Livingston,D.M. and Pavletich,N.P. (2002) Structure of the 53BP1 BRCT region bound to p53 and its comparison to the Brca1 BRCT structure. *Genes Dev.*, **16**, 583–593.

Jullien,D., Vagnarelli,P., Earnshaw,W.C. and Adachi,Y. (2002) Kinetochores localisation of the DNA damage response component 53BP1 during mitosis. *J. Cell Sci.*, **115**, 71–79.

Kraulis,P.J. (1991) MOLSCRIPT: a program to produce both detailed and schematic plots of protein structures. *J. Appl. Crystallogr.*, **24**, 946–950.

Krishnan,V.V., Thornton,K.H., Thelen,M.P. and Cosman,M. (2001) Solution structure and backbone dynamics of the human DNA ligase III α BRCT domain. *Biochemistry*, **40**, 13158–13166.

Lane,D.P. (1992) Cancer. p53, guardian of the genome. *Nature*, **358**, 15–16.

Laskowski,R.A., MacArthur,M.W., Moss,D.S. and Thornton,J.M. (1993) PROCHECK: a program to check the stereochemical quality of protein structures. *J. Appl. Crystallogr.*, **26**, 283–291.

Leslie,A.G.W. (1992) Molecular data processing. In Moras,D., Podjarny,A.D. and Thierry,J.C. (eds), *Crystallographic Computing 5*:

- From Chemistry to Biology*. Oxford University Press, Oxford, UK, pp. 50–61.
- Levine,A.J. (1993) The tumor suppressor genes. *Annu. Rev. Biochem.*, **62**, 623–651.
- McRee,D.E., (1999) XtalView/Xfi—a versatile program for manipulating atomic co-ordinates and electron density. *J. Struct. Biol.*, **125**, 156–165.
- Merritt,E.A. and Bacon,D.J. (1997) Raster3D photorealistic molecular graphics. *Methods Enzymol.*, **277**, 505–524.
- Nash,R.A., Caldecott,K.W., Barnes,D.E. and Lindahl,T. (1997) XRCC1 protein interacts with one of two distinct forms of DNA ligase III. *Biochemistry*, **36**, 5207–5211.
- Navaza,J. (1994) AMoRe: an automated package for molecular replacement. *Acta Crystallogr. A*, **50**, 157–163.
- Pavletich,N.P., Chambers,K.A. and Pabo,C.O. (1993) The DNA-binding domain of p53 contains the four conserved regions and the major mutation hot spots. *Genes Dev.*, **7**, 2556–2564.
- Rappold,I., Iwabuchi,K., Date,T. and Chen,J. (2001) Tumor suppressor p53 binding protein 1 (53BP1) is involved in DNA damage-signaling pathways. *J. Cell Biol.*, **153**, 613–620.
- Schultz,L.B., Chehab,N.H., Malikzay,A. and Halazonetis,T.D. (2000) p53 binding protein 1 (53BP1) is an early participant in the cellular response to DNA double-strand breaks. *J. Cell Biol.*, **151**, 1381–1390.
- Sibanda,B.L., Critchlow,S.E., Begun,J., Pei,X.Y., Jackson,S.P., Blundell, T.L. and Pellegrini,L. (2001) Crystal structure of an XRCC4–DNA ligase IV complex. *Nat. Struct. Biol.*, **8**, 1015–1019.
- Taylor,R.M., Wickstead,B., Cronin,S. and Caldecott,K.W. (1998) Role of a BRCT domain in the interaction of DNA ligase III- $\alpha$  with the DNA repair protein XRCC1. *Curr. Biol.*, **8**, 877–880.
- Thukral,S.K., Blain,G.C., Chang,K.K. and Fields S. (1994) Distinct residues of human p53 implicated in binding to DNA, simian virus 40 large T-antigen, 53BP1 and 53BP2. *Mol. Cell. Biol.*, **14**, 8315–8321.
- Williams,R.S., Green,R. and Glover,J.N. (2001) Crystal structure of the BRCT repeat region from the breast cancer-associated protein BRCA1. *Nat. Struct. Biol.*, **8**, 838–842.
- Xia,Z., Morales,J.C., Dunphy,W.G. and Carpenter,P.B. (2001) Negative cell cycle regulation and DNA damage-inducible phosphorylation of the BRCT protein 53BP1. *J. Biol. Chem.*, **276**, 2708–2718.
- Yamane,K. and Tsuruo,T. (1999) Conserved BRCT regions of TopBP1 and of the tumor suppressor BRCA1 bind strand breaks and termini of DNA. *Oncogene*, **18**, 5194–5203.
- Zhang,X. *et al.* (1998) Structure of an XRCC1 BRCT domain: a new protein–protein interaction module. *EMBO J.*, **17**, 6404–6411.

*Received March 1, 2002; revised and accepted May 28, 2002*